

This work has been submitted to the IEEE for possible publication. Copyright may be transferred without notice, after which this version may no longer be accessible.

arXiv:2312.17344v1 [math.DS] 28 Dec 2023

# Recursive Self-Composite Approach Towards Structural Understanding of Boolean Networks

Jongrae Kim, *Senior Member, IEEE*, Woojeong Lee, and Kwang-Hyun Cho, *Senior Member, IEEE*,

**Abstract**—Boolean networks have been widely used in many areas of science and engineering to represent various dynamical behaviour. In systems biology, they became useful tools to study the dynamical characteristics of large-scale biomolecular networks and there have been a number of studies to develop efficient ways of finding steady states or cycles of Boolean network models. On the other hand, there has been little attention to analyzing the dynamic properties of the network structure itself. Here, we present a systematic way to study such properties by introducing a recursive self-composite of the logic update rules. Of note, we found that all Boolean update rules actually have repeated logic structures underneath. This repeated nature of Boolean networks reveals interesting algebraic properties embedded in the networks. We found that each converged logic leads to the same states, called kernel states. As a result, the longest-length period of states cycle turns out to be equal to the number of converged logics in the logic cycle. Based on this, we propose a leaping and filling algorithm to avoid any possible large string explosions during the self-composition procedures. Finally, we demonstrate how the proposed approach can be used to reveal interesting hidden properties using Boolean network examples of a simple network with a long feedback structure, a T-cell receptor network and a cancer network.

**Index Terms**—Boolean networks, logic structures, kernel states, biological networks, systems biology

## I. INTRODUCTION

**B**OOLEAN network formalism is a useful mathematical modelling approach to describe complex interactions and dynamics of biological systems [1]. In this formalism, individual biological entities, such as genes, proteins, or other molecular components, are represented by nodes, while their interactions are depicted as edges. These nodes are assigned with time-varying binary states – either on (active) or off (inactive) – thus facilitating a simplified modelling process and allowing for a broader range of interactions while still capturing essential dynamical properties. Logical relationships among these nodes are specified through Boolean functions. Following these rules, node states are updated synchronously

or asynchronously, eventually converging to a stable state known as an attractor. It has been previously demonstrated that stable attractor states in gene regulatory networks correspond to distinct cellular phenotypes or cell fates [2]. In this regard, extensive studies have been done to investigate the long-term behaviour of biological networks represented by Boolean network models, aiming to predict real intra-cellular dynamics across various biological processes, including the cell cycle [3], differentiation [4], [5], and tumorigenesis [6], [7]. Such studies have not only enhanced our understanding of biological phenomena but also enabled the prediction of drug responses for precision medicine of complex diseases [8] and the identification of potential therapeutic targets for drug discovery [9], [10].

Let us consider the Boolean networks given by

$$\begin{aligned} x_1(k+1) &= f_1[x_1(k), x_2(k), \dots, x_{n-1}(k), x_n(k)] \\ x_2(k+1) &= f_2[x_1(k), x_2(k), \dots, x_{n-1}(k), x_n(k)] \\ &\vdots \\ x_n(k+1) &= f_n[x_1(k), x_2(k), \dots, x_{n-1}(k), x_n(k)] \end{aligned} \quad (1)$$

where  $x_i(k)$  is the  $i$ -th Boolean state equal to either *true* (equivalently T or 1) or *false* (equivalently F or 0) at  $k$  for  $i = 1, 2, \dots, n-1, n$ ,  $k$  is the non-negative integer in  $[0, \infty)$ ,  $x_i(0)$  is the initial state,  $f_i(\cdot)$  is a synchronous update rule consisting of the Boolean operations conjunction (and,  $\wedge$ ), disjunction (or,  $\vee$ ), and negation(not,  $\neg$ ) and  $x_i(k+1)$  is the updated Boolean state for  $i = 1, 2, \dots, n-1, n$ .

The Boolean network shown in (1) can be written in a compact form as follows:

$$\mathbf{x}(k+1) = \mathbf{f}[\mathbf{x}(k)] \quad (2)$$

where

$$\mathbf{x}(k) = [x_1(k) \quad x_2(k) \quad \dots \quad x_n(k)]^T \quad (3a)$$

$$\mathbf{f}[\mathbf{x}(k)] = [f_1[\mathbf{x}(k)] \quad f_2[\mathbf{x}(k)] \quad \dots \quad f_n[\mathbf{x}(k)]^T] \quad (3b)$$

and  $(\cdot)^T$  is the transpose.

The state space is  $2^n$ -dimensional and the main interest in Boolean network analysis is finding steady-states and periodic cycles. In the synchronous update of Boolean networks, every initial state converges to a steady state or a periodic cycle. As  $n$  increases, the dimension of the state space,  $2^n$ , increases exponentially. Therefore, executing the exhaustive search to find attractors is infeasible even for moderate-size networks, e.g.,  $n$  around 30. One of the well-known approaches in Boolean networks called the semi-tensor approach is also an

Manuscript received 26 December 2023. This work was supported by the Cheney Fellow program of the University of Leeds, U.K. It was also supported by the National Research Foundation of Korea (NRF) grants funded by the Korea Government, the Ministry of Science and ICT [2023R1A2C3002619 and 2021M3A9I4024447 (Bio & Medical Technology Development Program)] and the internal fund/grant of Electronics and Telecommunications Research Institute (ETRI) [23RB1100, Exploratory and Strategic Research of ETRI-KAIST ICT Future Technology].

J. Kim is with the School of Mechanical Engineering, University of Leeds, Leeds LS2 9JT, UK (e-mail: menjkim@leeds.ac.uk).

W. Lee is with the Department of Bio & Brain Engineering, KAIST, Daejeon, Republic of Korea (e-mail: frship35@kaist.ac.kr).

K-H. Cho is with the Department of Bio & Brain Engineering, KAIST, Daejeon, Republic of Korea (e-mail: ckh@kaist.ac.kr, Corresponding author).

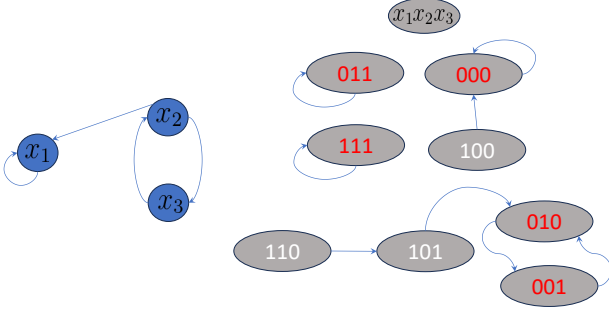


Fig. 1. The interaction graph and state transition map of the Boolean network, (4), are shown. There are three steady-states,  $\{s = (000), (011), (111)\}$  and one cycle with the period 2,  $\{s = (010) \leftrightarrow (001)\}$ , where  $s = (x_1x_2x_3)$ .

exhaustive method [11]. The aggregation algorithm proposed in [12] relies on the specific modular structure of the networks. Hence, Boolean network analysis results are often obtained from probabilistic approaches based on simulations over a finite number of random samples. Finding attractors or control strategies for Boolean networks is also known to be NP-hard [13].

On the other hand, there are rich theoretical results in the continuous system described by ordinary differential equations:  $dx/dt = f(x)$ , where  $d(\cdot)/dt$  is the derivative with respect to time,  $t$ , and  $f(x)$  is a nonlinear function satisfying the existence and uniqueness conditions of the solution. The equilibrium points and their stability are inherent properties of the right-hand side of the differential equation, i.e.,  $f(x)$ . The solution of  $f(x) = 0$  is the equilibrium point and the eigenvalues of  $df(x)/dx$  at the equilibrium point provide the stability condition. The main motivation of our approach to be shown is from the question about whether the right-hand side of (2), i.e.,  $f[x(k)]$ , can also provide any clue for the characteristics of Boolean networks.

In the following sections, first, the motivation of the proposed method is illustrated with a simple toy example. Secondly, we present the main results of the recursive self-composition approach to investigate the structure of Boolean networks. Thirdly, we apply the proposed method to various examples including a simple network with a long feedback path and two biological networks – a T-cell signalling pathway and a cancer signalling network – highlighting the advantages of the proposed method. Finally, the conclusions are made.

## II. RECURSIVE SELF-COMPOSITE BOOLEAN NETWORK

### A. Motivations

Let us consider the following Boolean network model:

$$x_1(k+1) = x_1(k) \wedge x_2(k) \quad (4a)$$

$$x_2(k+1) = x_3(k) \quad (4b)$$

$$x_3(k+1) = x_2(k) \quad (4c)$$

Since the right-hand side of  $x_1(k+1)$  in (4) is of the conjunction of  $x_1(k)$  and  $x_2(k)$ , the 75% of  $x_1(k+1)$  is 0 (False), i.e., the 25% of  $x_1(k+1)$  is 1 (True). All four possible outputs from the conjunction of  $x_1(k)$  and  $x_2(k)$  produce 0

except when both are 1. Using the same approach, examining the right-hand sides of  $x_2(k+1)$  and  $x_3(k+1)$  in (4), the probability that the output of  $x_2(k+1)$  or  $x_3(k+1)$  is 0 or 1 is 50%.

The question is how accurate these probabilities are with respect to the final state. The final state is a steady state or a state belonging to a cycle. Figure 1 shows the interaction graph and transition map, where the state,  $s$ , is equal to  $(x_1x_2x_3)$ . Three steady states and one cycle are shown in red. If we consider all eight states in Figure 1 and count the number of states with the final state  $x_1 = 1$ , there is only one case. In all other cases except  $(x_1x_2x_3) = (111)$ ,  $x_1$  becomes 0. Hence, the probability for  $x_1$  equal to 0 in the final state is 87.5%, 7 out of 8. It is not equal to the 75% that was estimated earlier.

The cause for this difference is the usage of one-step propagation equation. So, a longer propagation would provide better estimation. Any exact calculation can be done by exhaustive numerical simulation considering all possible states, which is not feasible for large-size networks. Instead, let us consider the two-step propagation symbolically as follows:

$$\begin{aligned} x_1(k+2) &= x_1(k+1) \wedge x_2(k+1) \\ &= [x_1(k) \wedge x_2(k)] \wedge x_3(k) \\ &= x_1(k) \wedge x_2(k) \wedge x_3(k) \end{aligned} \quad (5a)$$

$$x_2(k+2) = x_3(k+1) = x_2(k) \quad (5b)$$

$$x_3(k+2) = x_2(k+1) = x_3(k) \quad (5c)$$

Similarly, the three-step propagation is obtained as follows:

$$\begin{aligned} x_1(k+3) &= x_1(k+1) \wedge x_2(k+1) \wedge x_3(k+1) \\ &= [x_1(k) \wedge x_2(k)] \wedge x_3(k) \wedge x_2(k) \\ &= x_1(k) \wedge x_2(k) \wedge x_3(k) \end{aligned} \quad (6a)$$

$$x_2(k+3) = x_2(k+1) = x_3(k) \quad (6b)$$

$$x_3(k+3) = x_3(k+1) = x_2(k) \quad (6c)$$

The four-step propagation is given by

$$\begin{aligned} x_1(k+4) &= x_1(k+1) \wedge x_2(k+1) \wedge x_3(k+1) \\ &= x_1(k) \wedge x_2(k) \wedge x_3(k) \end{aligned} \quad (7a)$$

$$x_2(k+4) = x_3(k+1) = x_2(k) \quad (7b)$$

$$x_3(k+4) = x_2(k+1) = x_3(k) \quad (7c)$$

and it turns out that the five-step propagation is the same as the two-step propagation.

As shown in Figure 2, the update logic itself switches between the two update rules. While the  $x_2$  and  $x_3$  propagation rules cross-update between the two, the  $x_1$  update rule converges to the conjunction of the three states. By inspecting the right-hand side of the converged update rule, the probability of  $x_1$  converging to the final state equal to 0 is 7 out of 8, which coincides with the true probability.

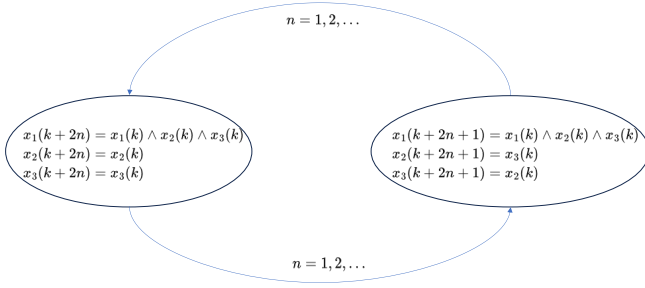


Fig. 2. The Boolean logic in (4) switches between two update rules.

In the exhaustive approach, the transition matrix,  $L$ , describes the updates of eight states in Figure 1 as follows:

$$\mathbf{s}_{k+1} = \underbrace{\begin{bmatrix} 1 & 0 & 0 & 0 & 0 & 0 & 0 & 0 \\ 0 & 0 & 1 & 0 & 0 & 0 & 0 & 0 \\ 0 & 1 & 0 & 0 & 0 & 0 & 0 & 0 \\ 0 & 0 & 0 & 1 & 0 & 0 & 0 & 0 \\ 1 & 0 & 0 & 0 & 0 & 0 & 0 & 0 \\ 0 & 0 & 1 & 0 & 0 & 0 & 0 & 0 \\ 0 & 0 & 0 & 0 & 0 & 1 & 0 & 0 \\ 0 & 0 & 0 & 0 & 0 & 0 & 0 & 1 \end{bmatrix}}_L \underbrace{\begin{bmatrix} (000) \\ (001) \\ (010) \\ (011) \\ (100) \\ (101) \\ (110) \\ (111) \end{bmatrix}}_{\mathbf{s}_k} \quad (8)$$

In the semi-tensor approach [11],  $\mathbf{s}_k$  or  $\mathbf{s}_{k+1}$  is the state vector with the element corresponding to the current state equal to 1 and the rest set to 0, i.e.,

$$\mathbf{s}_k = [s_0 \ s_1 \ \dots \ s_{2^n-1}]^T \quad (9)$$

where  $s_i = 1$  for  $i$  equal to the decimal number whose binary number corresponds to the current state  $(x_1 x_2 \dots x_n)$  and  $s_i = 0$  for the others, where  $i \in \{0, 1, 2, \dots, 2^n - 1\}$ . For instance, if the initial state for  $(x_1, x_2, x_3)$  is equal to (010), then,  $s_2 = 1$  and the rest of  $s_i$  equal to 0.

$$\mathbf{s}_0 = [0 \ 0 \ 1 \ 0 \ 0 \ 0 \ 0 \ 0]^T \quad (10)$$

(010), i.e.,  $s_2 = 1$ , is converted to (001), i.e.,  $s_1 = 1$ , as shown in Figure 1, and  $L\mathbf{s}_0$  provides the corresponding transition state,  $\mathbf{s}_1$ , i.e.,

$$\mathbf{s}_1 = [0 \ 1 \ 0 \ 0 \ 0 \ 0 \ 0 \ 0]^T \quad (11)$$

Further iterations reveal that  $L^{2k} = L^2$  and  $L^{2k+1} = L^3$  for  $k = 1, 2, \dots$ . Hence, the algorithms constructed in [11] can find all steady states and cycles by inspecting  $L^2$  and  $L^3$ . However, one of the main drawbacks of this approach is the requirement for *always* checking all  $2^n$  states to construct  $L$ . Hence, the algorithm is limited to solving only small or moderate-size Boolean networks only.

On the other hand, the approach we propose does not require explicitly checking  $2^n$  states or constructing the matrix  $L$ . As shown in Figure 2, the recursive self-composition provides the converged cyclic logic without checking the  $2^3$  states.

## B. Main Results

*Assumption 1 (Synchronous Update):* All states in the Boolean network given by (2) are updated synchronously. The states in the right-hand-side of (2) is the one at the same step.

*Definition 1 (Recursive Self-Composite):* The  $p$ -times recursive self-composite of the Boolean network is given by

$$\begin{aligned} \mathbf{x}(p) &= \mathbf{f}[\mathbf{x}(p-1)] = \mathbf{f}[\mathbf{f}[\mathbf{x}(p-2)]] = \dots \\ &= \mathbf{f}[\mathbf{f}[\mathbf{f}[\dots[\mathbf{f}(\mathbf{x}(0))]]]] \\ &= \underbrace{\mathbf{f} \circ \mathbf{f} \circ \mathbf{f} \circ \dots \circ \mathbf{f}}_{p\text{-times}}[\mathbf{x}(0)] = \mathbf{f}^p[\mathbf{x}(0)] \end{aligned} \quad (12)$$

where  $p$  is a positive integer.

*Theorem 1 (Convergence of Recursive Self-Composition):* All recursive self-composition of the synchronous Boolean network given by (2) converges to a steady-state logic or a cyclic logic, i.e.,

$$\mathbf{f}^{p^*+r}(\mathbf{x}) = \mathbf{f}^{p^*+r+\ell^*}(\mathbf{x}) \quad (13)$$

where  $p^*$  between 0 and  $2^n$  is the minimum number of recursions when the logic starts repeating itself,  $r$  is a non-negative integer and  $\ell^*$  between 1 and  $2^n$  is the period of logic cycles.

*Proof:* Deterministic synchronous update Boolean networks have a finite number of states, i.e.,  $2^n$ , any initial state repeats the same state at longest in  $2^n + 1$  steps. It is guaranteed at least  $\mathbf{x}(2n+1)$  is equal to  $\mathbf{x}(p)$  for  $1 \leq p \leq 2^n$ . As  $\mathbf{x}(2n+1) = \mathbf{f}^{2n+1}[\mathbf{x}(0)]$  and  $\mathbf{x}(p) = \mathbf{f}^p[\mathbf{x}(0)]$ ,  $\mathbf{f}^p[\mathbf{x}(0)] = \mathbf{f}^{2n+1}[\mathbf{x}(0)]$  and  $p$  is between 1 and  $2^n$ . Hence,  $p^*$  always exists between 1 and  $2^n$ .

Assuming that the smallest  $\ell^*$  is strictly greater than  $2^n$  leads to a contradiction with the finite number of states  $2^n$ . Therefore,  $\ell^*$  must be between 0 (for the cases of no periodic cycles but only steady states) and  $2^n$ . ■

When  $\ell^*$  is equal to 0, it corresponds to the case that there is only one steady-state logic. If  $\ell^*$  is equal to 3, three update rules switch between them. For instance, the Boolean network given in (4) has  $p^*$  equal to 2, when the logic repetition begins to start, and  $\ell^*$  equal to 2, which is the period of logic cycles.

*Remark 1:* In the worst case, if  $p^*$  is equal to  $2^n$ , the computational cost to find a repeating logic is at least as much expensive as the exhaustive search.

*Theorem 2 (Longest Cycle Upper Bound):* All cycle lengths of every Boolean logic cannot be longer than the length of the converged logic cycle,  $\ell^*$ .

*Proof:* Let us assume there exists a cycle of the period,  $m$ , strictly longer than  $\ell^*$ . Let  $\mathbf{s}_{p^*}$  be the state for the first time arrived in the cycle at  $p^*$ -step from the state  $\mathbf{s}_{p^*-1}$ , which is not in the cycle, and the cycle propagates as follows:

$$\begin{array}{ccccccc} \mathbf{s}_{p^*-1} & \xrightarrow{L} & \mathbf{s}_{p^*} & \xrightarrow{L} & \mathbf{s}_{p^*+1} & \xrightarrow{L} & \mathbf{s}_{p^*+2} \\ & & & & & & \downarrow L \\ \mathbf{s}_{p^*+\ell^*} & \xleftarrow{L} & \mathbf{s}_{p^*+\ell^*+1} & \xleftarrow{L} & \dots & \xleftarrow{L} & \mathbf{s}_{p^*+3} \\ & & L \downarrow & & & & \\ \mathbf{s}_{p^*+\ell^*+1} & \xrightarrow{L} & \dots & \xrightarrow{L} & \mathbf{s}_{p^*+m-1} & \xrightarrow{L} & \mathbf{s}_{p^*} \end{array}$$

where  $\mathbf{s}_{p^*}$  in the last line is equal to the one in the first line and the cycle repeats. By the definition of cycle,  $\mathbf{s}_i \neq \mathbf{s}_j$  for

$i \neq j$ . Also, notice that as  $s_{p^*+m} = s_{p^*}$  and  $\mathbf{f}^{p^*+m}(\mathbf{x}_0) = \mathbf{f}^{p^*}(\mathbf{x}_0) = \mathbf{x}_0$ ,  $m$  must be an integer multiple of  $\ell^*$ .

We can re-write  $(p^* + \ell^* + 1)$ -step using the composition logic as follows:

$$s_{p^*+\ell^*+1} = Ls_{p^*+\ell^*} \rightarrow \mathbf{x}(p^* + \ell^* + 1) = \mathbf{f}^{p^*+\ell^*+1}[\mathbf{x}(0)]$$

where  $\mathbf{x}(p^* + \ell^* + 1)$  corresponds to  $s_{p^*+\ell^*+1}$ . By Theorem 1, the following equality satisfies

$$\mathbf{f}^{p^*+\ell^*+1}[\mathbf{x}(0)] = \mathbf{f}^{p^*+1}[\mathbf{x}(0)] \quad (14)$$

Hence,

$$s_{p^*+\ell^*+1} = s_{p^*+1} \quad (15)$$

This contradicts  $s_i \neq s_j$  for  $i \neq j$  in the cycle. Therefore, no cycle can have a longer period than  $\ell^*$ . ■

*Definition 2 (Kernel States Set):* The kernel states set,  $\mathbb{K}$ , of the synchronous Boolean network, (2), includes all steady-states and the states belonging to cycles.

For instance, all the states indicated in red in Figure 1 are the kernel states of the network and  $\mathbb{K} = \{(000), (001), (010), (011), (111)\}$  or equivalently  $\mathbb{K} = \{s_0, s_1, s_2, s_3, s_7\}$ .

*Theorem 3 (Kernel States Set of Converged Logic):* The one-step propagated state,  $\mathbf{x}(1)$ , by the converged logic in (13), i.e.,  $\mathbf{x}(1) = \mathbf{f}^{p^*+r}[\mathbf{x}(0)]$ , converges the same kernel states set of the original Boolean network for any fixed non-negative integer  $r$ .

*Proof:* If a steady-state is absent in the kernel set of a converged logic, then it contradicts the property of steady-states. Hence, the proof for steady-states cases becomes trivial. Let us consider a cycle of the period,  $\ell^*$ , as follows:

$$\begin{array}{c} \overbrace{s_0 \rightarrow s_1 \rightarrow s_2 \rightarrow \dots \rightarrow s_{\ell^*}} \\ \underbrace{Ls_0 \quad Ls_1 \quad Ls_2 \quad \dots \quad Ls_{\ell^*-1}} \end{array} \quad (16)$$

Let the initial state,  $\mathbf{x}(0)$ , correspond to  $s_0$ . And, it propagates  $p^*$  steps as follows:

$$\begin{aligned} \mathbf{x}_1 &= \mathbf{f}[\mathbf{x}(0)] \rightarrow \mathbf{x}_2 = \mathbf{f}^2[\mathbf{x}(1)] \rightarrow \dots \\ \dots &\rightarrow \mathbf{x}_{p^*} = \mathbf{f}^{p^*}[\mathbf{x}(p^* - 1)] \end{aligned} \quad (17)$$

As  $\mathbf{x}(0)$  starts in the cycle, all propagated states are in the cycle. Hence,  $\mathbf{x}_{p^*}$  is equal to one of the states in the cycle. Specifically,  $\mathbf{x}_{p^*}$  is equal to the state corresponding to  $s_{r^*}$ , where  $r^* = p^* - \ell^*q$ , which is in  $[0, \ell^*]$ ,  $q$  is the maximum integer such that  $\ell^*q$  is less than or equal to  $p^*$ .

Without loss of the generality, let us assume that  $r^*$  is equal to 2, i.e.,  $\mathbf{x}_{p^*}$  corresponds to  $s_2$ . It implies that:  $s_2$  is an element of the kernel state set of  $\mathbf{f}^{p^*}$ ,  $s_3$  is an element of the kernel state set of  $\mathbf{f}^{p^*+1}$  and so forth.

Let us choose the initial state,  $\mathbf{x}(0)$  corresponding to  $s_1$  and repeat the same procedure. Then,  $r^*$  becomes 3 and this results in:  $s_3$  is an element of the kernel state set of  $\mathbf{f}^{p^*}$ ,  $s_4$  is an element of the kernel state set of  $\mathbf{f}^{p^*+1}$  and so forth.

For the shorter cycles less than the period  $\ell^*$ , the same steps provide the proof that all the cycle states must be in the kernel

state of each of the converged logic. Therefore, the converged logic includes all states in the cycles. ■

*Theorem 4 (Longest Length Cycle):* There exists at least one cycle whose length is equal to the period of the logic cycle,  $\ell^*$ .

*Proof:* By Theorem 3, the range set of every converged logic is identical with each other as the kernel set,  $\mathbb{K}$ . Hence, once the logic converges to the logic cycle, whose period is  $\ell^*$ , the mapping from  $\mathbb{K}$  to  $\mathbb{K}$  repeats  $\ell^*$  times. Each of the mappings must be different from each other. Otherwise, the existence of the logic cycle equal to  $\ell^*$  is violated. In addition, due to the periodicity of the logic cycles, the  $\ell^*$ -th mapping brings the states back to the states mapped by the first logic cycle. ■

*Definition 3 (Kernel Logic):* The Kernel logic,  $\mathbf{f}^{p^*+k^*}$  is the converged logic having the same steady states and cycles as the original Boolean logic, where  $k^*$  is an integer between 0 and  $\ell^* - 1$ .

For instance, the converged logic in the right-hand side of Figure 2 has the same three steady states and one cycle as the original network given by (4).

*Theorem 5 (Existence of Kernel Logic):* For every Boolean network, there exists at least one kernel logic among the converged logic cycles.

*Proof:* Given that there are  $\ell^*$  number of converged logic,  $\mathbf{f}^{p^*+k}$ , where  $k$  is an integer from 0 to  $\ell^* - 1$ , take  $n$ -time self composites for a fixed  $k$  logic as follows:

$$\underbrace{\mathbf{f}^{p^*+k} \circ \dots \circ \mathbf{f}^{p^*+k} \circ \mathbf{f}^{p^*+k}}_{t\text{-times}}[\mathbf{x}(0)] = \mathbf{f}^{t(p^*+k)}[\mathbf{x}(0)] \quad (18)$$

$p^* + k$  can be expressed as

$$p^* + k = m\ell^* + r \quad (19)$$

where  $m$  is the largest integer satisfying  $p^* + k \geq m\ell^*$ , where  $r$  can be any integer between 0 and  $\ell^* - 1$  as  $k$  is between 0 and  $\ell^* - 1$ . Set  $r = 1$  and multiply  $t$ , which is an integer,

$$t(p^* + k) = tml^* + t \quad (20)$$

Hence, we can cover all integers from 0 to  $\ell^* - 1$  by varying  $t$ . Therefore, it covers all  $\ell^*$  cyclic logic and there exists always at least one kernel logic. ■

*Remark 2 (Leaping & Filling):* One of the ways to speed up the self-composition iteration and possibly increase the chance to avoid large string-length explosions is leaping by performing larger-step composition instead of a one-step composition. First,

$$\mathbf{x}(k+2) = \mathbf{f}^2[\mathbf{x}(k)] = \mathbf{g}[\mathbf{x}(k)]$$

is obtained. Secondly,

$$\mathbf{x}(k+4) = \mathbf{g}[\mathbf{x}(k+2)] = \mathbf{g}^2[\mathbf{x}(k)] = \mathbf{h}[\mathbf{x}(k)]$$

then,

$$\mathbf{x}(k+8) = \mathbf{h}[\mathbf{x}(k+4)] = \mathbf{h}^2[\mathbf{x}(k)]$$

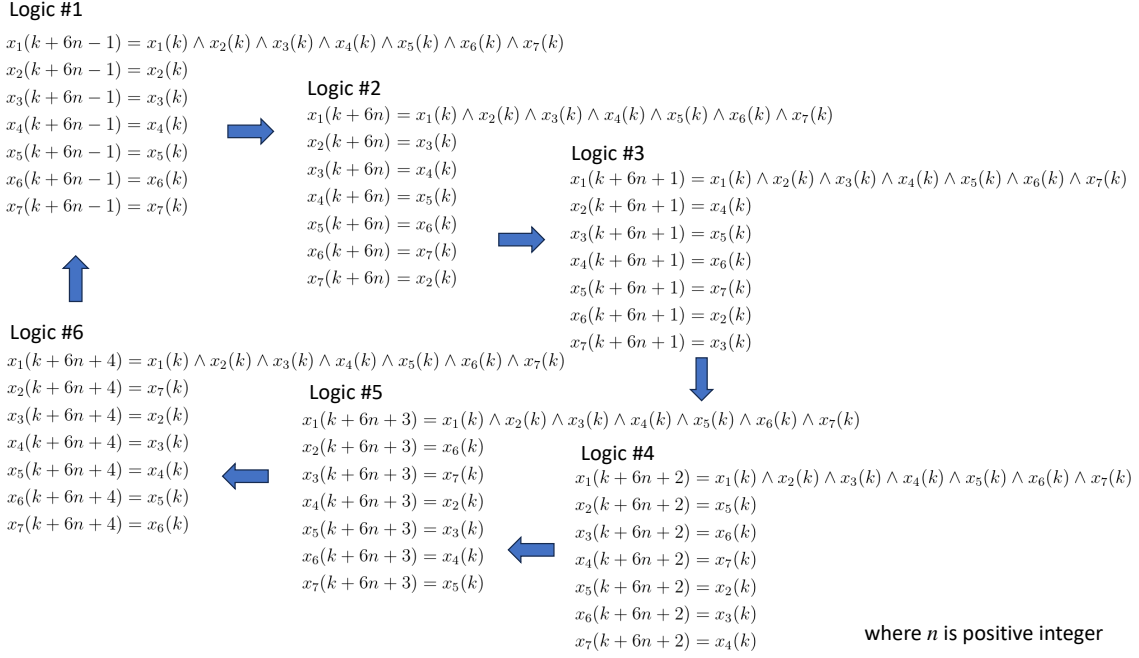


Fig. 3. The Boolean logic in (21) cycles between six update rules.

and we continue until the logic converges. Once the logic converges, we apply  $f(\cdot)$  repeatedly and obtain the logic between the leaps. For instance,  $\mathbf{h}[\mathbf{x}(k)]$  converges and  $\mathbf{h}^2[\mathbf{x}(k)]$  is equal to  $\mathbf{h}[\mathbf{x}(k)]$ . Then, the logic for  $\mathbf{x}(k+5)$ ,  $\mathbf{x}(k+6)$  and  $\mathbf{x}(k+7)$  are obtained by the filling sequence as follows:

$$\begin{aligned} \mathbf{x}(k+5) &= \mathbf{f}[\mathbf{x}(k+4)] = \mathbf{f}\{\mathbf{h}[\mathbf{x}(k)]\} \\ \mathbf{x}(k+6) &= \mathbf{f}[\mathbf{x}(k+5)] = \mathbf{f}^2\{\mathbf{h}[\mathbf{x}(k)]\} \\ \mathbf{x}(k+7) &= \mathbf{f}[\mathbf{x}(k+6)] = \mathbf{f}^3\{\mathbf{h}[\mathbf{x}(k)]\} \end{aligned}$$

### III. EXAMPLES

*Example 1 (Longer feedback network):* The following Boolean network is an extended network of (4) having a longer feedback chain between  $x_2$  and  $x_7$ :

$$x_1(k+1) = x_1(k) \wedge x_2(k) \quad (21a)$$

$$x_2(k+1) = x_3(k) \quad (21b)$$

$$x_3(k+1) = x_4(k) \quad (21c)$$

$$x_4(k+1) = x_5(k) \quad (21d)$$

$$x_5(k+1) = x_6(k) \quad (21e)$$

$$x_6(k+1) = x_7(k) \quad (21f)$$

$$x_7(k+1) = x_2(k) \quad (21g)$$

By the recursive compositions, the logic converges at  $p^* = 5$  to the cyclic logic whose period,  $\ell^*$ , is equal to 6 as shown in Figure 3. It has three steady-states, a cycle with period 2, two cycles with period 3 and nine cycles with period 6. The number of elements in the kernel states set is 65 ( $= 3 + 1 \times 2 + 2 \times 3 + 9 \times 6$ ). Among the six logics in the cycle, Logic #2 and #6 in Figure 3 are the kernel logic. By inspecting the right-hand side of the converged logic, the common characteristics found are as follows:  $x_1$  equal to 1 is a rare event, and the other states

equal to 0 or 1 have the same chance. This coincides with the fact that there is only one kernel state with  $x_1$  equal to 1 among the 65 kernel states. Hence, we would be able to design numerical and lab experiments to find rare events, which would be challenging to find even in numerical experiments based on Monte Carlo type random simulations.

*Example 2 (T-cell receptor network):* A T-cell receptor Boolean network model in [14] having 37 states with 3 control inputs is given by

$$\begin{aligned} \text{AP1}(k+1) &= \text{Fos}(k) \wedge \text{Jun}(k), \quad \text{Ca}(k+1) = \text{IP3}(k) \\ \text{CalcIn}(k+1) &= \text{Ca}(k), \quad \text{cCbl}(k+1) = \text{ZAP70}(k) \\ \text{CRE}(k+1) &= \text{CREB}(k), \quad \text{CREB}(k+1) = \text{Rsk}(k) \\ \text{DAG}(k+1) &= \text{PLCg}^*(k), \quad \text{ERK}(k+1) = \text{MEK}(k) \\ \text{Fos}(k+1) &= \text{ERK}(k) \\ \text{Fyn}(k+1) &= [\text{Lck}(k) \wedge \text{CD45}(k)] \\ &\quad \vee [\text{TCR}^+(k) \wedge \text{CD45}(k)] \\ \text{Gads}(k+1) &= \text{LAT}(k), \quad \text{Grb2SOS}(k+1) = \text{LAT}(k) \\ \text{IKKbeta}(k+1) &= \text{PKCth}(k), \quad \text{IP3}(k+1) = \text{PLCg}(\text{act})(k) \\ \text{Itk}(k+1) &= \text{SLP76}(k) \wedge \text{ZAP70}(k) \\ \text{IkB}(k+1) &= \neg \text{IKKbeta}(k), \quad \text{JNK}(k+1) = \text{SEK}(k) \\ \text{Jun}(k+1) &= \text{JNK}(k), \quad \text{LAT}(k+1) = \text{ZAP70}(k) \\ \text{Lck}(k+1) &= \neg \text{PAGCsk}(k) \wedge \text{CD45}(k) \wedge \text{CD4}(k) \\ \text{MEK}(k+1) &= \text{Raf}(k), \quad \text{NFAT}(k+1) = \text{CalcIn}(k) \\ \text{NFkB}(k+1) &= \neg \text{IkB}(k), \quad \text{PKCth}(k+1) = \text{DAG}(k) \\ \text{PLCg}^*(k+1) &= [\text{Itk}(k) \wedge \text{PLCg}^+(k) \wedge \text{SLP76}(k) \\ &\quad \wedge \text{ZAP70}(k)] \vee [\text{PLCg}^+(k) \wedge \text{Rlk}(k) \\ &\quad \wedge \text{SLP76}(k) \wedge \text{ZAP70}(k)] \end{aligned}$$

$$\begin{aligned}
\text{PAGCsk}(k+1) &= \text{Fyn}(k) \vee \neg \text{TCR}^+(k) \\
\text{PLGg}^+(k+1) &= \text{LAT}(k), \text{Raf}(k+1) = \text{Ras}(k) \\
\text{Ras}(k+1) &= \text{Grb2Sos}(k) \vee \text{RasGRP1}(k) \\
\text{RasGRP1}(k+1) &= \text{DAG}(k) \wedge \text{PKCth}(k) \\
\text{Rlk}(k+1) &= \text{Lck}(k), \text{Rsk}(k+1) = \text{ERK}(k) \\
\text{SEK}(k+1) &= \text{PKCth}(k), \text{SLP76}(k+1) = \text{Gads}(k) \\
\text{TCR}^+(k+1) &= \neg \text{cCbl}(k) \wedge \text{TCRlig}(k) \\
\text{TCR}^\dagger(k+1) &= \text{Fyn}(k) \vee [\text{Lck}(k) \wedge \text{TCR}^+(k)] \\
\text{ZAP70}(k+1) &= \neg \text{cCbl}(k) \wedge \text{Lck}(k) \wedge \text{TCR}^\dagger(k)
\end{aligned}$$

where  $(\cdot)^+$  represents the binding status,  $(\cdot)^*$  denotes being activated,  $(\cdot)^\dagger$  indicates phosphates, CD45, CD4 and TCRlig are the three control inputs and there are four biomolecular species to be considered as the outputs of the networks, which are API, CRE, NFAT and NFkB. In [15]<sup>1</sup>, this T-cell Boolean network was used for structural controllability analysis to design a feedback controller.

*Case 1* (CD45=1, CD4=1, TCRlig=1): API and NFAT converges to 0, NFkB converges to 1 and CRE switches between the following update rules: If  $n$  is even and greater than or equal to 4,

$$\begin{aligned}
\text{CRE}(k+n) &= \text{Lck}(k) \wedge \text{TCR}^\dagger(k) \wedge \neg \text{cCbl}(k) \\
&\wedge [\text{PAGCsk}(k) \vee \text{ZAP70}(k) \vee \neg \text{Fyn}(k)] \\
&\wedge [\text{PAGCsk}(k) \vee \text{ZAP70}(k) \vee \neg \text{TCR}^+(k)] \quad (22)
\end{aligned}$$

and if  $n$  is odd and greater than or equal to 5,

$$\begin{aligned}
\text{CRE}(k+n) &= \text{cCbl}(k) \wedge \text{PAGCsk}(k) \wedge \neg \text{ZAP70}(k) \\
&\wedge [\text{Fyn}(k) \vee \neg \text{TCR}^+(k)] \quad (23)
\end{aligned}$$

Based on this finding, an additional feedback control input would be designed to derive CRE towards desired states. A total of 21 states update logic out of the 37 states converge to a period of 2 switching logic. The rest 16 states converge to steady states of either 0 or 1. The state space shrinks from  $2^{37}$  (137 billion) to  $2^{21}$  (2 million), which is only 0.0015% of the original size of the state space.

*Case 2* (at least one of CD45, CD4 or TCRlig equal to 0): API, CRE and NFAT converge to 0 and NFkB converges to 1. There is no possibility of introducing further control structures to change the outputs.

These analyses lead the problem space from originally computationally infeasible to feasible ranges. In addition, they clearly show what states can or cannot be controlled and what the update-rule structures of states to be controlled are.

From a biological perspective, when foreign antigens are presented to T cell receptors (TCR) and co-receptors (CD4), along with the involvement of receptor-type protein tyrosine phosphatase (CD45) [14], this triggers an immune response signaling cascade that includes the Ras-Raf-Mek-Erk pathway. This, in turn, leads to the transcriptional activation of numerous immune-related genes, such as IL-2, IL-6, IL-10, TNF- $\alpha$ , and others [16]. The promoters of these genes commonly contain a DNA target sequence known as the cAMP-responsive

element (CRE), to which transcription factors belonging to the CREB family (CREB) can specifically bind and initiate transcription.

To counterbalance the risk of an overactive immune response that could potentially result in autoimmunity, a negative feedback mechanism is in place. This mechanism is primarily mediated by the E3 ubiquitin ligase (cCbl) [17], which facilitates the degradation of key signaling proteins, including the activated protein tyrosine kinase (ZAP70), thereby ensuring immune response homeostasis [14]. Within the T-cell receptor network, with all control inputs set to 1, a negative feedback loop between cCbl and ZAP70 continuously operates, resulting in oscillations between the states (cCbl=0, ZAP70=1) and (cCbl=1, ZAP70=0). In the former states, according to the Boolean logic, TCR<sup>+</sup>, Fyn, PAGCsk, Lck, and TCR<sup>†</sup>, which also form feedback regulations to ZAP70, attain values of 1, 1, 0, 1, and 1, respectively, while in the latter states, 0, 0, 1, 0, and 0, respectively. In the former scenario, ZAP70 gets activated by the feedback regulations and gives a positive signal to the downstream Ras-Raf-Mek-Erk pathway, leading to the activation of CRE. Rather, in the latter scenario, ZAP70 gets inactivated, so that CRE also switches back to the inactive state. As a result, the long-term dynamics of CRE exhibit a switching behavior between 0 and 1, signifying that the T cell signalling cascade effectively orchestrates immune responses without straying into an excessive territory, thereby maintaining immune homeostasis.

This regulatory process corresponds to the results of *Case 1* (CD45=1, CD4=1, TCRlig=1), where the recursive self-composite logic of CRE switches between (22) and (23). In (22) and (23), Ras-Raf-Mek-Erk pathway between CRE and upstream feedback loops is omitted, while only the feedback regulations are represented as a switching for the presence or absence of the negation operator in front of cCbl(k), ZAP70(k), and Fyn(k). In the results of *Case 2*, on the other hand, when any one of the input controls equals to 0, multiple feedback loops will no longer be able to operate, leading to ZAP70 keeping inactivated so that CRE converges to 0. This signifies that the immune response signalling cascade is deactivated, rendering the homeostatic effect of negative feedback unnecessary.

In summary, we showed that the recursive self-composite logics of CRE, (22) and (23), serve as an intuitive representation of the long-term oscillatory dynamics of the output of the T cell Boolean network model.

*Example 3 (Cancer signaling network)*: In the study by Fumiã et al. [6], a Boolean network model was developed to represent human tumorigenesis. This model encompasses 90 states of proteins within cancer signaling pathways, alongside 6 control inputs – Mutagen, GFs (growth factors), Nutrients, TNF $\alpha$ , Hypoxia and Gli. The Boolean functions in the network were initially formulated using algebraic operators (+, -) and sgn( $\cdot$ ) – a thresholding function in which  $\text{sgn}(x) = 0$  for  $x \leq 0$  and 1 for  $x > 0$ . As this algebraic representation is less straightforward for recursive self-composition, we opted to transform the Boolean functions into an equivalent form utilizing the Boolean operations, while preserving their orig-

<sup>1</sup>The T-cell model in [15] adopted from [14] includes a few typos.

inal truth tables, the Boolean model is available to download as indicated in Supplementary Material.

The network outputs include two bio-molecules, Glut1 and Lactic acid, as well as two virtual nodes that represent cellular phenotypes – Apoptosis and DNA repair. In addition, the other cellular phenotype, Proliferation, was defined by examining the long-term dynamics of the network, particularly the activation sequence of cyclin nodes. In [18], attractor-transition analysis of this network was carried out to investigate the critical transition of tumorigenesis along with the accumulation of driver mutations.

The update logic for Cyclins D has the longest string. Its update rule has 23k characters. And, the first three self-compositions make the length increase exponentially, i.e., 149k, 34M and 293M. Applying the self-composition procedure to the original network produces long string chains of the updated rules. The lengths of the strings are too long to be handled by most digital computers. As analyzing Boolean networks are known to be an NP-hard problem [13], finding some networks producing large string beyond the current computer calculation speed and memory capacity is not surprising.

To restrict the network to the condition with normoxic (normal oxygen level), sufficient growth factors and nutrient-rich five input states are set as follows: Mutagen = 0, GFs = 1, Nutrients = 1, TNF $\alpha$  = 0, Hypoxia = 0 and Gli = 0. In [6], it is shown that the cell enters into the proliferation cycle with a period of 7.

p53, Cyclins A and Cyclins D are identified by trial and error as the additional control inputs to change the phenotype. Pinning the three states to 1 and applying the self-compositions make the logic length become too large again before it converges.

By applying the leaping every 4 iterations, i.e., starting from  $\mathbf{x}(k+1)$ , we obtain  $\mathbf{x}(k+2)$ ,  $\mathbf{x}(k+3)$ ,  $\mathbf{x}(k+4)$  and  $\mathbf{x}(k+5)$ . Then, leaping from  $\mathbf{x}(k+5)$ , we obtain  $\mathbf{x}(k+10)$ ,  $\mathbf{x}(k+15)$  and  $\mathbf{x}(k+20)$ , and it converges at  $\mathbf{x}(k+15)$ . And, applying the filling procedure from  $\mathbf{x}(k+16)$  to  $\mathbf{x}(k+19)$  we confirm the logic converges to a single logic.

The maximum string length of the updated rules for each iteration is as follows: 17k, 29k, 60k, 65k, 64k, 10 and 10, where the corresponding longest string states are TSC1/2, Cytoc/APAF1, Cytoc/APAF1, GSH, eEF2k, E2F and E2F, respectively. It converges to a steady state instead of the cycle and the phenotype changes from proliferation to apoptosis. More interestingly, all states converge to 0 or 1 regardless of the initial conditions except E2F( $k+15$ ), a transcription factor for cell-cycle regulation genes, which converges to

$$E2F(k+15) = E2F(k) \wedge [\neg Rb(k)]$$

where Rb is retinoblastoma protein.

The example demonstrates the power of the proposed method in finding a hidden simple logic behind the complex networks. Such finding can help to identify further important drug target candidates to be developed for efficient cancer therapeutic strategies.

## IV. CONCLUSIONS & FUTURE WORKS

We present the recursive self-composite approach to reveal the hidden characteristics of Boolean networks. Most interestingly, we found the cyclic nature of synchronous Boolean update rules. This is the first time that the converging nature of the Boolean logic dynamics is unveiled explicitly. We also found several interesting properties of the converged logic: the existence of kernel logic and its relationship with the length of periodic cycles in the state space. There might be many other interesting hidden structures of the Boolean network, which we aim to reveal in future studies using the recursive self-composite approach. Finding fundamental relationships between the repeating logic and biological phenomena to control the behaviour of Boolean networks and extending the approaches to asynchronous Boolean networks are of immediate interest.

## SUPPLEMENTARY MATERIAL

The Boolean network model of the cancer signalling network in Python is available to download at the following link: [https://github.com/myjr52/Fumia\\_cancer\\_network\\_boolean\\_model](https://github.com/myjr52/Fumia_cancer_network_boolean_model)

## ACKNOWLEDGMENT

The authors would like to thank the support of the Cheney fellowship. The research was initiated in June 2023 by the visit of KHC to the University of Leeds as one of the Cheney fellowship activities, hosted by JK.

## REFERENCES

- [1] S. Kauffman, “Homeostasis and differentiation in random genetic control networks,” *Nature*, vol. 224, no. 5215, pp. 177–178, 1969.
- [2] S. Huang, G. Eichler, Y. Bar-Yam, and D. E. Ingber, “Cell fates as high-dimensional attractor states of a complex gene regulatory network,” *Physical Review Letters*, vol. 94, no. 12, p. 128701, 2005.
- [3] Ö. Sahin, H. Fröhlich, C. Löbke, U. Korf, S. Burmester, M. Majety, J. Mattern, I. Schupp, C. Chaouiya, D. Thieffry *et al.*, “Modeling erbb receptor-regulated g1/s transition to find novel targets for de novo trastuzumab resistance,” *BMC Systems Biology*, vol. 3, no. 1, pp. 1–20, 2009.
- [4] S. Collombet, C. Van Oevelen, J. L. Sardina Ortega, W. Abou-Jaoudé, B. Di Stefano, M. Thomas-Chollier, T. Graf, and D. Thieffry, “Logical modeling of lymphoid and myeloid cell specification and transdifferentiation,” *Proceedings of the National Academy of Sciences*, vol. 114, no. 23, pp. 5792–5799, 2017.
- [5] A. Carbo, R. Hontecillas, B. Kronsteiner, M. Viladomiu, M. Pedragosa, P. Lu, C. W. Philipson, S. Hoops, M. Marathe, S. Eubank *et al.*, “Systems modeling of molecular mechanisms controlling cytokine-driven cd4+ t cell differentiation and phenotype plasticity,” *PLoS Computational Biology*, vol. 9, no. 4, p. e1003027, 2013.
- [6] H. F. Fumiã and M. L. Martins, “Boolean network model for cancer pathways: predicting carcinogenesis and targeted therapy outcomes,” *PLoS One*, vol. 8, no. 7, p. e69008, 2013.
- [7] S.-H. Cho, S.-M. Park, H.-S. Lee, H.-Y. Lee, and K.-H. Cho, “Attractor landscape analysis of colorectal tumorigenesis and its reversion,” *BMC Systems Biology*, vol. 10, pp. 1–13, 2016.
- [8] M. Choi, J. Shi, Y. Zhu, R. Yang, and K.-H. Cho, “Network dynamics-based cancer panel stratification for systemic prediction of anticancer drug response,” *Nature Communications*, vol. 8, no. 1, p. 1940, 2017.
- [9] S. R. Choi, C. Y. Hwang, J. Lee, and K.-H. Cho, “Network analysis identifies regulators of basal-like breast cancer reprogramming and endocrine therapy vulnerability,” *Cancer Research*, vol. 82, no. 2, pp. 320–333, 2022.



- [10] N. Kim, C. Y. Hwang, T. Kim, H. Kim, and K.-H. Cho, "A cell-fate reprogramming strategy reverses epithelial-to-mesenchymal transition of lung cancer cells while avoiding hybrid states," *Cancer Research*, vol. 83, no. 6, pp. 956–970, 2023.
- [11] D. Cheng and H. Qi, "A linear representation of dynamics of boolean networks," *IEEE Transactions on Automatic Control*, vol. 55, no. 10, pp. 2251–2258, 2010.
- [12] Y. Zhao, J. Kim, and M. Filippone, "Aggregation algorithm towards large-scale boolean network analysis," *IEEE Transactions on Automatic Control*, vol. 58, no. 8, pp. 1976–1985, 2013.
- [13] T. Akutsu, M. Hayashida, W.-K. Ching, and M. K. Ng, "Control of boolean networks: Hardness results and algorithms for tree structured networks," *Journal of Theoretical Biology*, vol. 244, no. 4, pp. 670–679, 2007.
- [14] S. Klamt, J. Saez-Rodriguez, J. A. Lindquist, L. Simeoni, and E. D. Gilles, "A methodology for the structural and functional analysis of signaling and regulatory networks," *BMC bioinformatics*, vol. 7, pp. 1–26, 2006.
- [15] S. Zhu, J. Lu, S.-i. Azuma, and W. X. Zheng, "Strong structural controllability of boolean networks: Polynomial-time criteria, minimal node control, and distributed pinning strategies," *IEEE Transactions on Automatic Control*, vol. 68, no. 9, pp. 5461–5476, 2023.
- [16] A. Y. Wen, K. M. Sakamoto, and L. S. Miller, "The role of the transcription factor creb in immune function," *The Journal of Immunology*, vol. 185, no. 11, pp. 6413–6419, 2010.
- [17] L. Duan, A. L. Reddi, A. Ghosh, M. Dimri, and H. Band, "The cbl family and other ubiquitin ligases: destructive forces in control of antigen receptor signaling," *Immunity*, vol. 21, no. 1, pp. 7–17, 2004.
- [18] H. Chu, D. Lee, and K.-H. Cho, "Precritical state transition dynamics in the attractor landscape of a molecular interaction network underlying colorectal tumorigenesis," *PLoS One*, vol. 10, no. 10, p. e0140172, 2015.